JOURNAL OF COMPUTATIONAL PHYSICS 31, 42–59 (1979)

Numerical Solution of the Helmholtz Equation for Two-Dimensional Polygonal Regions*†

ROBERT J. RIDDELL, JR.

Lawrence Berkeley Laboratory, University of California, Berkeley, California 94720

Received May 4, 1976; revised May 3, 1978

The Helmholtz equation together with associated boundary conditions can be solved using a dipole distribution on the boundary of any region of interest. If the region has corners, the distribution satisfies a singular integral equation. In this paper numerical techniques for the solution of this equation which take into account the analytic properties of the solution are discussed. Although a complete error analysis has not been developed, some indicators of the errors generated are considered. The technique is illustrated by comparing the numerical solution of the eigenvalue problem associated with various two-dimensional polygonal regions with exact solutions. Numerical solutions of the Dirichlet problem for the Helmholtz equation are also obtained. A method for eliminating difficulties arising from nearby singularities is also implemented, and sample results given.

I. INTRODUCTION

In a previous article, hereafter designated I, we have analyzed the solution of the Helmholtz equation in terms of a boundary dipole distribution, D, for two-dimensional regions with corners [1]. It was shown that D satisfies a singular integral equation which incorporates the boundary conditions imposed on the solution of the Helmholtz equation. Using techniques which have been developed for such singular equations, it was demonstrated that $D(s)$ in the vicinity of a corner can be expanded in powers (typically fractional) of s, where s is the distance from the corner. The specific powers needed in the expansion depend on the angle at the corner. Further, if the boundary condition is an analytic function of s near $s = 0$, many of the powers can be summed to yield Bessel functions, and $D(s)$ can then be expanded in a series of Bessel functions.

These ideas have been developed for use in a computer program which can produce very accurate solutions of the Helmholtz equation; in this paper we will describe some of the techniques which were employed, as well as give a description of the results obtained for some particular cases. We have applied the methods to two different kinds of problem: first, we have obtained eigenvalues and eigensolutions for various two-dimensional polygons; and, second, we have obtained solutions of some sample

* This work was supported by the U.S. Department of Energy.

† The U.S. Government's right to retain a nonexclusive royalty-free license in and to the copyright covering this paper, for governmental purposes, is acknowledged.

0021-9991/79/040042-18$02.00/0

boundary value problems for such figures. In the latter case, numerical difficulties can arise as a result of the presence of nearby eigenvalues of the homogeneous integral equation; we have implemented techniques for dealing with this situation which were developed in I.

The integral equation discussed in I, Eq. (I.4) has a kernel function which incorporates the Hankel function, $H_1^{(1)}(\kappa \mid \mathbf{r} - \mathbf{r}' \mid)$, as a factor. (All references to equations in I will be in the form: Eq. (I.N), where N is the particular equation in that paper.) With that choice, solutions of the Helmholtz equation for scattered waves, $\psi(\mathbf{r})$, on the outside of a closed boundary will automatically satisfy an outgoing wave condition as $r \to \infty$. On the other hand, if one is dealing with a finite region, so that the asymptotic boundary condition is of no importance, a simpler choice for the kernel can be made in which $H_1^{(1)}$ is replaced by iN_1, where N_1 is the Neumann function of order one. This has the advantage that the kernel of the integral equation becomes real so that $D(s)$ can be chosen to be real. Thus for computational purposes the number of unknowns can be reduced by a factor of two. For practical calculations there would be a disadvantage as well: It is well known that the Helmholtz equation has no eigensolutions if the solution satisfies an outgoing-wave boundary condition at infinity, but it does have eigensolutions if the sinusoidal asymptotic behavior implied by the choice of iN_1 rather than $H_1^{(1)}$ in the kernel is made. As a result, eigensolutions of the exterior problem must be considered if one wishes to obtain an accurate solution of the interior problem. This is the converse of the well-known difficulty discussed in I in which an interior "partner" eigensolution can generate a pole in the solution of an exterior problem at an internal eigenvalue. For the purposes of this paper, however, the presence of these "spurious" eigensolutions is an advantage, since we wish to demonstrate the effectiveness of the ideas developed in I for the solution of numerical problems. As was discussed there, when solving external problems the internal eigensolutions will be present even for the Hankel-function kernel, but the methods for dealing with them are no different from those to be given here. Thus for the computations of this paper we have chosen to use the Neumann function in the kernel, so that the integral equation to be solved for $D(s)$ is:

$$\psi_C(s) = \frac{D(s)}{2} - \frac{\kappa}{4} \oint_C D(s') \frac{N_1(\kappa \mid \mathbf{r}' - \mathbf{r} \mid)}{\mid \mathbf{r}' - \mathbf{r} \mid} (r' - r) \cdot d\sigma', \tag{1}$$

where $\psi_C(s)$ is the boundary value of $\psi(\mathbf{r})$ on the boundary, C, of the region.

In I it was shown that Eq. (1) is a singular equation at a corner of the boundary, and that the solution, $D(s)$, can be divided into an even and an odd function near the corner, each of which can be expanded in a series of powers of s; i.e.,

$$D(s) = \sum a_n s^{\xi_n}, \tag{2}$$

where there are two sequences for each type of symmetry at the corner. Specifically, for the even solution, $D_+(s)$:

$$\xi_n^{(+)} = \frac{(2n-1)\,\pi}{\alpha}, \frac{(2n-2)\,\pi}{(2\pi - \alpha)}, \tag{3}$$

where α is the corner angle, and for the odd one, $D_-(s)$:

$$\xi_n^{(-)} = \frac{2n\pi}{\alpha}, \frac{(2n-1)\,\pi}{(2\pi-\alpha)}, \tag{4}$$

where n takes on all positive integral values. Further, a series of powers of even integral spacing is generated beginning with each of the above ξ_n's, which in many cases can be summed to produce Bessel functions, with the result that

$$D(s) = \sum d_n J_{\xi_n}(\kappa s). \tag{5}$$

These results are complete if $\psi_C(s)$ is an analytic function of s in the neighborhood of $s = 0$, but if $\psi_C(s)$ has a branch point at $s = 0$, then additional terms would be generated in $D(s)$ which could not be so simply expressed. In this paper we will choose $\psi_C(s)$ to be analytic so that Eq. (5) is valid.

II. Numerical Technique

We have developed an approximation technique for the solution of Eq. (1) for arbitrary polygons where the sides are straight line segments, and for which $D(s)$ near a corner has the behavior specified by Eq. (5). To reduce the integral equation to an approximate finite form we first introduced a set of points, $\mathbf{r}_k$, on the boundary for which $D(s_k)$ was to be obtained. Then to decrease the number of points used, the distribution was "mirrored" about one side, thus automatically guaranteeing that $\psi(\mathbf{r}) = 0$ there. No distribution is needed on that side.

A. *Corner treatment*

Near a corner we chose N_c points spaced equidistantly on each side of the corner in addition to the corner point itself. Identical treatment on the two sides of a corner greatly facilitated the separation of $D(s)$ into $D_+(s)$ and $D_-(s)$. Some consideration of other than uniform point spacing was made, but no particularly suitable choice seemed indicated. A choice of points analogous to that made in Gaussian integration does not seem to apply here since we are not dealing with an analytic function, and furthermore since $\mathbf{r}$ appears as a parameter in the integration over $\mathbf{r}'$, one might wish to have different points for each $\mathbf{r}$. The actual corner spacing, h_c, was fixed as

$$h_c = \{\ell/[N_d - 2(N_c - 2)]\} \cdot (2/N_c)\, h_f,$$

where ℓ is the length of the side, N_d is the number of points on the side, and h_f is a free parameter. Thus if $h_f = 1$, h_c is chosen so that the corner points cover a space equivalent to 2 average steps in the remainder of the side, and if $N_c = 2$ will be simply ℓ/N_d. This choice was made to allow simple variation in the number of terms in the corner expansions leaving the mid-range points unaffected.

Once the choice of N_c was made, it was then assumed that the $D_{\pm}(s)$ could be expanded as:

$$D_{+}(s) = \sum_{n=1}^{N_c+1} d_n^{(+)} J_{\xi_n^{(+)}}(\kappa s)$$

and

$$D_{-}(s) = \sum_{n=1}^{N_c} d_n^{(-)} J_{\xi_n^{(-)}}(\kappa s)$$

where the set of ξ's was chosen to be the lowest $N_c + 1$ elements from Eq. (3) or the lowest N_c elements from Eq. (4). With the set of points and ξ_n's chosen, the expansion coefficients were determined by solving the equations:

$$D(s_i) = \sum_{j=1}^{N_c} d_j J_{\xi_j}(\kappa s_i) \qquad i = 1, 2, \ldots, N_c , \tag{6}$$

so that the d_j's could be expressed in terms of the $D(s_i)$'s.

These expansions were then used to obtain the integral of the kernel function times D over a region from the corner to the beginning of the mid-range region which will be described later.

The function $N_1(x)$ which appears in the kernel can be conveniently divided into three parts [2]:

$$N_1(x) \equiv -2/(\pi x) + (2/\pi) \log x \cdot J_1(x) + \phi(x).$$

Each of these parts was given a different numerical treatment. A typical integral over the first term involves

$$I(\mathbf{r}, a, \xi) = \int_0^a \frac{r \sin\theta \cdot s^{\xi}\, ds}{r^2 - 2rs\cos\theta + s^2},$$

where (r, θ) are the polar coordinates of the point $\mathbf{r}$ in a system of coordinates centered at the corner and with θ as the angle between $\mathbf{r}$ and the side of interest. This integral can easily be converted to

$$I(\mathbf{r}, a, \xi) = \operatorname{Im}\left\{\int_0^a \frac{s^{\xi}\, ds}{s - re^{i\theta}}\right\},$$

and if $r > a$

$$I(\mathbf{r}, a, \xi) = -a^{\xi} \operatorname{Im}\left\{\sum_{n=0}^{\infty} \frac{[a/(re^{i\theta})]^{n+1}}{n + \xi + 1}\right\}. \tag{7}$$

For $r > a$, this series can be used to evaluate the integral, although for $r \sim a$ convergence is poor and an alternative form shown in Appendix A was then used. For

$r < a$ the series is divergent but we can obtain its analytic continuation if we first observe that [3]:

$$\int_0^a \frac{s^\xi\, ds}{s+z} = \frac{a^{\xi+1}}{(\xi+1)\,z}\,{}_2F_1\left(1,\,\xi+1;\,\xi+2;\,-\frac{a}{z}\right),$$

where ${}_2F_1$ is the ordinary hypergeometric function. This expression can be converted into a form useful for computation by using the Kummer relation [4]:

$${}_2F_1\left(1,\,\xi+1;\,\xi+2;\,-\frac{a}{z}\right) = \frac{(\xi+1)}{\xi}\left(\frac{z}{a}\right){}_2F_1\left(1,\,-\xi;\,1-\xi;\,-\frac{z}{a}\right) - \frac{\pi(\xi+1)}{\sin\pi\xi}\left(\frac{z}{a}\right)^{\xi+1}.$$

The hypergeometric function on the right-hand side can be expanded in a power series in (z/a). To obtain an integral over $J_\xi(\kappa s)$ rather than s^ξ, we simply expanded J_ξ in a power series in s.

The second term in the expression for $N_1(x)$ includes the factors $\log x$ and $J_1(x)$, where $x \equiv (s^2 - 2rs\cos\theta + r^2)^{1/2}$. Since $J_1(x)/x$ is an even function of x, the square root in x does not produce any singularity, and we simply expanded the Bessel function, keeping only a few terms in the power series. On the other hand, the logarithmic factor can be converted into terms like those previously discussed via an integration by parts. Thus, for example,

$$\int_0^a s^\xi \log(s^2 - 2rs\cos\theta + r^2)\, ds = \frac{a^{\xi+1}}{\xi+1}\log(a^2 - 2ar\cos\theta + r^2) - \frac{2}{\xi+1}\int_0^a \frac{s^{\xi+1}(s - r\cos\theta)}{s^2 - 2rs\cos\theta + r^2}\, ds.$$

The third term in N_1, $\phi(x)$, is odd in x and an entire function. It was therefore expressed as a polynomial and integrated directly.

B. *Mid-range treatment*

For the remaining points on a side, the spacing was chosen to vary linearly from the corner points to the center of the side. This provided some flexibility so that more points could be chosen either near a corner or near the center of a side as desired, or one could chose a uniform spacing. The parameters were so chosen that the first point away from the N_c corner points would fit as if the corner had two such steps times a free parameter, g_f, while the linear variation in step spacing was chosen in such a way that half the steps on a side would cover half of the side. After some experimenting with g_f, it was generally found that the results for $g_f = 1$ seemed to be satisfactory, and the calculations reported in this paper were made with this choice.

For the mid-range integrals, since $\mathbf{r}'$ is not near a corner, the integrand has no singularity in $D(s')$, while the principal value integral is zero for a straight side which includes $\mathbf{r} = \mathbf{r}'$. Thus we assumed that in this mid-range case the entire integrand

could be well approximated by a polynomial of finite degree, and we used a three-point Lagrangian interpolation approximation which was integrated analytically. To minimize truncation error the integration was divided into subpieces of which each had an integration region chosen to be symmetric about the central point, thereby eliminating contributions from cubic terms in the integrand. If the step size between points was constant, each sub-integration was carried out from half a step on one side of the center point to half a step on the other side. For nonconstant steps a generalization of this idea was used which still retained the symmetry.

This technique may be contrasted with that used to produce Simpson's rule. In that case, one uses the value of the integrand at three points to construct an approximating quadratic form which is then integrated over the entire region covered by the three points. If one wishes to integrate over a larger region, the next sub-region would include the integrand at the end-point of the sub-region just integrated. In our approximation the approximating quadratic form is constructed as for Simpson's rule, but the integration is only carried out for half a step on either side of the central point, and on moving on to the next sub-region two of the preceding values of the function plus one new evaluation are used to produce the next quadratic approximation. In both techniques the lowest order truncation error is proportional to the quartic term in a Taylor expansion of the function in a sub-region, but one easily finds the magnitude of such errors is reduced by a factor of 16 in our method as compared with the use of Simpson's rule as described.

For uniform step size, our explicit integration formula is easily found to be:

$$\int_{s_n-h/2}^{s_n+h/2} f(s')\,ds' \cong \frac{h}{24}\,[f(s_{n-1}) + 22f(s_n) + f(s_{n+1})].$$

This approximation, or its generalization for nonuniform steps, was used to integrate over each sub-region with a mid-range point as the center. A 4-point interpolation formula to include cubic terms was also tried; in this case errors similar to those found with the 3-point formula were obtained.

By using these techniques the integral equation was reduced to an approximate set of linear, algebraic equations which could then be solved for $D(s_k)$ using standard methods. This approach has been used to find the eigenvalues of the Laplacian for a variety of polygonal regions. The eigenvalues were determined by finding approximate zeros of the determinant of these equations. Unfortunately, the kernel in the integral equation involves the eigenvalue, κ, in a complicated way, and so an iterative approach for finding κ was necessary.

III. Residual Errors

If the technique presented here is to be useful for the solution of practical problems, it seems very desirable to have an estimate of the accuracy achieved for various choices of the parameters in a particular calculation. The method has been applied

to find a few eigenvalues for problems with known analytic solutions and this is of course helpful. On the other hand, the eigenvalue as calculated here does not satisfy an extremum condition, and we will see that by varying the parameter N_c, for example, κ can change from below the correct value to above it. Thus it is very desirable to have some other criterion of accuracy for a solution, presumably one which is more closely related to the solution, $\psi(\mathbf{r})$.

Unfortunately, the system is quite complicated and we have not succeeded in developing a satisfactory overall error analysis. As a rough check we have used the methods described above to calculate the value of $\psi(\mathbf{r})$ at points on the boundary halfway between the points at which $D(s)$ was fixed in the equation. In the eigenvalue problem, the exact solution of the equation would give $\psi(\mathbf{r}) = 0$ on the boundary, so that the calculated $\psi(\mathbf{r})$ directly represents the error. For the inhomogeneous cases, we have an exact solution for $\psi(\mathbf{r})$ and again we can compute the errors present. We will call these calculated errors the "residual errors" in ψ. There is one difficulty with this calculation: Although the integral term in the equation can be calculated in exactly the same fashion regardless of where the point $\mathbf{r}$ is located, the term $D(s)/2$ cannot. This term is used in solving the integral equation for D at precisely the original points used, but it must be deduced by interpolation or otherwise at the "halfway" residual points. Thus there is a potential for error generation in the residual ψ calculation which is not present in the original approximating equation. At any rate, the same ideas for the evaluation of $D(s)$ were used for this purpose as went into the original approximating scheme so the result should be meaningful. In particular, for points near a corner we used expansions for $D(s)$ as given by Eq. (5), but in the mid-range, $D(s)$ was interpolated using a 6-point formula after a 4-point formula was found to produce a substantially larger residual ψ.

IV. Results

A. *Eigensolutions*

A program has been developed which incorporates the above ideas and it has been applied to a variety of problems, many of which have known analytic eigenfunctions. We present in Table I numerical results obtained for eigenvalues of a variety of figures, most of which can also be obtained analytically, as given in Appendix B. As has been mentioned already, we have chosen to generate $\psi(\mathbf{r})$ by $D(s)$ together with its mirror image as reflected in one side of the figure considered. It is found that results for incompletely symmetric figures, such as the 30°–60°–90° triangle thereby become dependent on which side is used for the reflecting. Thus, in Table I, an indication is stated as to which side was used for the reflection. In this Table, the results were obtained using 5 points near each corner to determine the expansion in powers of $J_\xi(\kappa s)$, and the parameter h_f was chosen to be 0.7. A total of 53 points was used on the boundary to express $D(s)$. For each figure, the longest side was chosen to have unit length.

TABLE I

Calculated Eigenvalues for Various Figures

Case	Refl. Side	κ	Error
Equilateral Triangle	Any	7.255218413	2.09×10^{-5}
45°–45°–90°	Long Side	9.934553774	-3.45×10^{-5}
	Short Side	9.933726725	-8.62×10^{-4}
30°–60°–90°	Long Side	11.08250598	8.80×10^{-6}
	Middle Side	11.08234583	-1.51×10^{-4}
	Short Side	11.08187715	-6.20×10^{-4}
Square	Any	4.442863599	-1.93×10^{-5}
"L"	Long Side	3.104787987	2.51×10^{-5}

Included in the table is an eigenvalue for an L-shaped region made up of three unit squares. This figure cannot be treated analytically, but there is extensive literature regarding numerical calculations for it. A very accurate technique has been developed by Fox, Henrici and Moler [5] for the determination of the eigenvalue, and they find $\kappa \cong 3.1047905$. Their value is used in computing the error of our calculation in the table. These authors note that their method, which is very effective for this particular problem, is not particularly better than other methods for other configurations. In comparison with the accuracy achieved using the boundary distribution, we would note the finite difference calculations of Reid and Walsh [6] in which they obtained

TABLE II

Eigenvalues for an Equilateral Triangle.
In all cases $h_f = 0.7$

N_d	N_c	κ	Error
22	3	7.255132500	-6.50×10^{-5}
24	4	7.255185579	-1.19×10^{-5}
26	5	7.255218413	2.10×10^{-5}
28	6	7.255240509	4.30×10^{-5}
36	5	7.255192079	-5.38×10^{-6}
46	5	7.255195141	-2.32×10^{-6}
		* * * * * * *	
26	5	7.084741761	("External" case)
26	5	11.08269983	2.03×10^{-4}

$\kappa = 3.1102$ using 360 points in the region and a 5-point formula. J. A. George [7], taking advantage of the symmetry and using a sophisticated finite element technique leading to 210 equations with a bandwidth of 101, obtained the value $\kappa = 3.1051$. To obtain our result we used 131 points on the boundary of the region and we took no account of symmetry. Thus in principle we could have reduced the number of equations by a factor of about two. Our accuracy seems the more impressive when it is reiterated that the eigenvalue does not satisfy a variational principle in this calculation.

In Table II, we show similar results for an equilateral triangle for a variety of parameters, N_c, and N_d. In this table we include one higher eigenvalue. The latter is in good agreement with the eigenvalue found in Table I for the 30° 60° 90° triangle. We also give an eigenvalue for the "partner" exterior problem which leads to a null interior solution for $\psi(\mathbf{r})$.

In this table it is seen that the accuracy of the eigenvalue, κ, is greatly enhanced by increasing N_d. The dependence of κ on N_c is not particulary marked, but it will be seen later that the residual $\psi(\mathbf{r})$ can be substantially improved as N_c is increased. Because of the way in which the parameters enter in the determination of points, the mid-range points are essentially unaffected if $N_d - 2N_c$ is kept fixed. This explains the particular choice made for N_d in the table. The parameter h_f affects primarily the step size in the corner region; as it is decreased the steps there are decreased proportionately. Since the mid-range points near the corner are linked to the corner points, they are similarly affected. On the other hand, if g_f is varied the corner points are unaffected while the mid-range points are modified. Evidently if either h_f or g_f is reduced the steps near the corners are reduced and so the steps in the middle of a side will be increased. For the choice of these two parameters we have typically found that values larger than 1.0 produced less satisfactory results than did smaller values, with the choice $h_f = 0.7$, $g_f = 1.0$ usually producing an approximately optimal κ and residual ψ. In all of the calculations reported here we have made this choice.

TABLE III

Non-Mirror Corner Expansion Coefficients*

N_d	N_c	d_0	$d_{1.2}$	$d_{2.4}$	$d_{3.0}$	$d_{3.6}$	$d_{4.8}$	$d_{6.0}$
22	3	−0.1494318	2.0224	7.612	2.375			
24	4	−0.1494461	2.0211	8.246	−3.970	16.61		
26	5	−0.1494549	2.0228	7.901	−2.411	19.66	−81.0	
28	6	−0.1494609	2.0236	7.520	0.822	16.93	−301.	2725.
36	5	−0.1494514	2.0228	7.886	−3.223	29.98	−262.	
46	5	−0.1494737	2.0232	7.759	−1.395	24.95	−348.	

* The Bessel functions in the expansion for $D(s)$ have been multiplied by a factor $(2/\kappa)^{\xi}\Gamma(\xi + 1)$ so that the coefficients in Tables III and IV directly give the coefficient of the lowest power, s^{ξ}, for each term.

TABLE IV

Mirror Corner Expansion Coefficients

N_d	N_c	$d_{0.75}$	$d_{2.25}$	$d_{3.0}$	$d_{3.75}$	$d_{5.25}$	$d_{6.0}$
22	3	1.039986	10.529	2.190			
24	4	1.039703	10.707	−0.306	9.367		
26	5	1.039696	10.683	0.065	7.508	15.49	
28	6	1.039697	10.618	1.947	−9.896	780.7	−2844.
36	5	1.039728	10.694	−0.227	9.986	−35.84	
46	5	1.039864	10.695	−0.252	10.694	−79.31	

In Tables III and IV we present for an equilateral triangle calculated values for the expansion coefficients of $D_+(s)$ at the corner not on the "mirror" side and $D_-(s)$ at the "mirror" corner, respectively. (We intentionally used an unsymmetric calculation to obtain $D(s)$ so that we could get an indication of the errors present in our treatment. In fact, $D_-(s)$ at the non-mirror corner was found to be very small.) The values of $D(s)$ were fixed by normalizing the distribution to have a maximum value of unity, as projected numerically using a quadratic approximation near the maximum.

It is seen that for all cases the first two coefficients are very well determined by the calculation and the third is still quite good. The remaining terms show considerably more variation, especially when they represent the last term in the series, but even those seem to show some convergence as the calculation is refined by using larger N_c , N_d . This behavior can be contrasted with results obtained using the expansion in powers, Eq. (2). In the latter situation, higher terms in the Bessel series are treated as unrelated to lower ones and so for given N_c the highest power included is often not very large. Further, one often finds powers in the series which are quite close in value and, as the behavior of such terms will be very similar in a limited region of s, the determination of the individual coefficients is much less precise. Thus the individual coefficients in the series of powers are much more erratic as parameters are changed, and they show much less tendency to converge as the calculation is refined.

Finally for the eigensolution problem, we present in the figures some results for the residual $\psi(\mathbf{r})$ as obtained using various choices for the parameters. In each case we have superimposed on the figure the solution for $D(s)$ as a smooth curve. In these calculations the ψ's are normalized by calculating the value of the solution at the center of the triangle using the dipole integral representation and then normalizing $D(s)$ so that the central value for ψ equals one.

In Fig. 1 we present the results for cases in which $N_d = 26, 36, 46$ with $N_c = 5$, to illustrate the decline of the residual error in ψ as the number of points is increased. Near the center of the side it is found that the ψ's decrease with N_d approximately as $\sim(N_d - 2N_c)^{-6}$. On the other hand, the large ψ's observed nearer the corners only decrease slowly with increasing N_d . These large residual errors involve interpolation

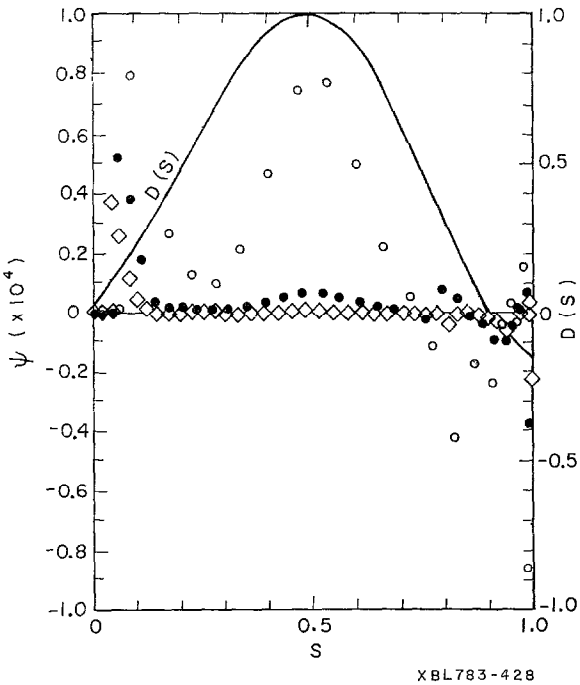

FIG. 1. Residual errors, $\psi(\mathbf{r})$, on the boundary of an equilateral triangle: $N_0 = 26$ (○), 36 (●), 46 (◇). The continuous curve gives $D(s)$.

of $D(s)$ in the integral equation using the 6-point Lagrange interpolation formula. Numerical estimates of the accuracy of this scheme when applied to analytic functions of the proper form for $D(s)$ suggest that the interpolation error agrees well with the calculated ψ. In the "transition region" near a corner $D(s)$ is not approximated with great accuracy either by the Lagrange formula or by the Bessel series expansion, the latter leading to still larger values for ψ. The difficulty with the Lagrange formula comes from the fact that there is a singularity at $s = 0$, and the region over which $D(s)$ is required to be approximated by a polynomial for the calculation of $\psi(\mathbf{r})$ near the corner is not small compared to the distance to the singularity. In fact, one of the points used even lies outside the radius of convergence of an infinite power series. On the other hand, interpolation formulas using fewer points, thereby reducing the interpolation region, give poorer results, so the illustrated results show the best we obtained.

In Fig. 2 similar results are given for points near a mirror corner, in which the number of points in the corner expansion was varied, keeping $N_d - 2N_c$ fixed. It is seen that the residual error, ψ, is substantially reduced by increasing N_c from 3 to 4. The improvement in going to $N_c = 5$ is fairly small, while there is not much to choose between $N_c = 5$ and $N_c = 6$. In any case, the errors in this region are quite small compared to those in the transition region. In Fig. 3, corresponding results are given

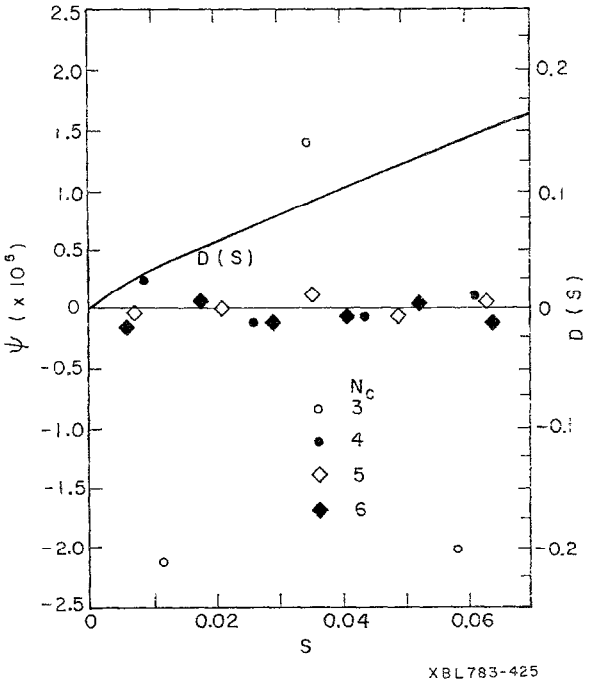

FIG. 2. Residual errors, $\psi(\mathbf{r})$, for an equilateral triangle near a mirror corner. The continuous curve gives $D(s)$.

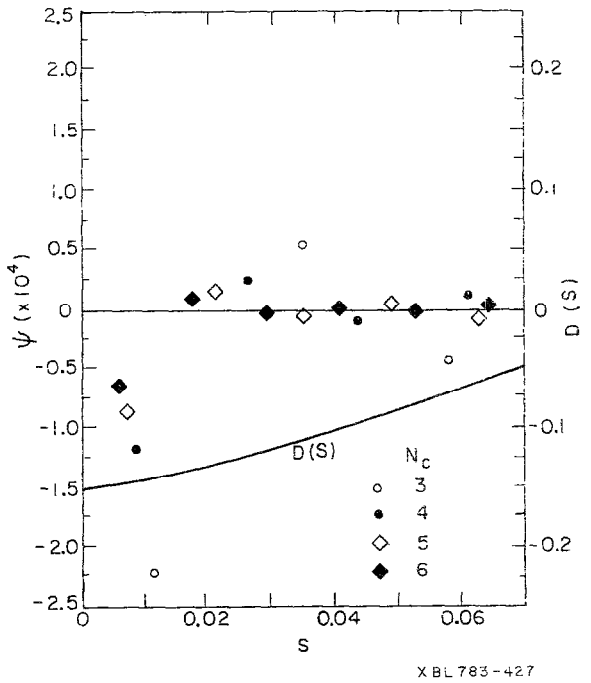

FIG. 3. Residual errors, $\psi(\mathbf{r})$, and $D(s)$ as in Fig. 2, but for the non-mirror corner.

for ψ's near the non-mirror corner. Here again the ψ's decrease as N_c is increased, although the last two choices, 5 and 6, are comparable.

As was pointed out in the introduction, our integral equation can have both "internal" eigensolutions of the Helmholtz equation and "external" eigensolutions. In addition to the internal eigenvalues, κ, given in Table I, we have also obtained external eigenvalues, κ_0. One example of the latter is given in Table II, and it is seen that the external eigenvalue is quite close to the internal one. Proximity of the eigenvalues is also found for the other figures in Table I. As a consequence, the eigensolutions, $D_\kappa(s)$ and $D_{\kappa_0}(s)$, are quite similar. (This result is very different from that found for an ordinary Fredholm equation: there the eigensolutions in a nondegenerate case are orthogonal. The difference has to do with the way in which the eigenvalue enters the kernel of the integral equation.) Since the eigenvalues are close together, one might expect that the technique developed in I for alleviating difficulties from nearby singularities could be used here to improve the eigensolution calculation. This can indeed be done, although a slight modification from the treatment in I is necessary.

The discussion in I relates to the solution of an inhomogeneous equation, and leads to Eq. (I.27). In that case we wrote $D \equiv A\,D_0 + D_1$, and the parameter A was fixed so that $\int_0^L D_1(s)g(s)\,ds = 0$. This was possible because the inhomogeneous equation for D_1 had two parts, one of which came from the inhomogeneous part of the equation for D. Since the latter term does not occur in the homogeneous case, the integral is

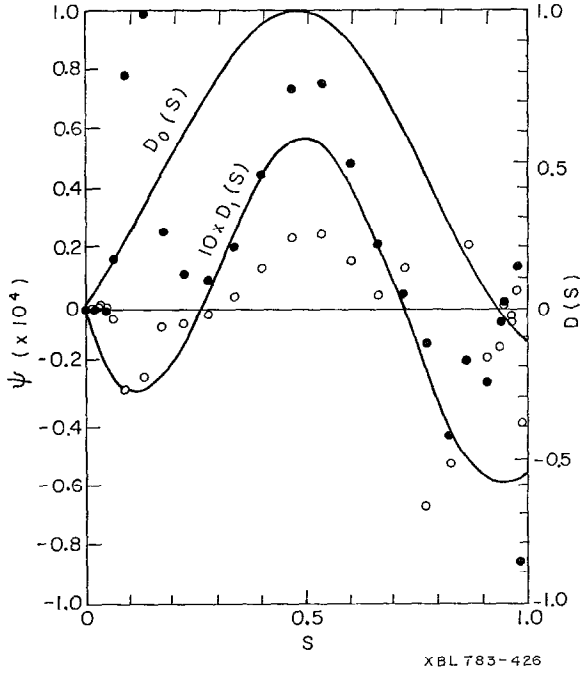

FIG. 4. Residual errors, $\psi(r)$, for the modified treatment (○) compared to the unmodified one

now proportional to A, and the eigenvalue condition is that the integral must vanish. For A we have simply chosen the value one. This idea has been implemented, using $g(s) = 1$, but no significant improvement for the eigenvalue was achieved. On the other hand, the large term $K_0 D_0$ in the expression for $\psi(\mathbf{r})$, Eq. (I.29), can be dropped, as was shown in I, so that errors in the calculation generated through this term will not occur in ψ. In Fig. 4 we present results obtained for the modified calculation. Since D_1 turns out to be much smaller than D_0 we have plotted D_0 and $10 \times D_1$. The residual errors, ψ, obtained for both the unmodified and modified treatments are given, and it is seen that for the latter the errors are significantly reduced.

distribution technique as used here: The calculation eigensolution will be small if an eigenvalue for the uninteresting "partner" problem is nearby. In the case presented here, we are interested in obtaining an eigensolution for an interior Dirichlet problem in a case in which there is a nearby eigenvalue, κ_0, of the exterior Neumann "partner" problem. Since the boundary distribution for the latter produces $\psi_0(\mathbf{r}) = 0$ in the interior region and both $D(s)$ and the kernel, K, for the representation of $\psi(\mathbf{r})$ will only differ from D_0 and K_0, respectively, by terms of order $(\kappa - \kappa_0)$, the desired interior eigensolution will be of the same order. Thus there must be substantial cancellations in the calculation of ψ, leading to a larger relative error than might otherwise be expected. For example, if $D(s)$ is normalized to have a maximum value of unity on the boundary of the equilateral triangle, the calculated eigensolution at the center of the equilateral triangle is only $\simeq 0.072$. The residual error ψ's have been calculated using a $D(s)$ normalized so that the solution for $\psi(\mathbf{r})$ at the center of the triangle is unity, and this helps to explain the large errors found for ψ as compared with the error in the eigenvalues, κ. Of course the exterior eigenvalue could be avoided if the kernel in I using a Hankel function were substituted for the choice made here, and it could be hoped that the cancellations in the calculation of $\psi(\mathbf{r})$ from $D(s)$ would not then be so significant.

B. *Inhomogeneous problems*

In addition to obtaining eigensolutions for the Helmholtz equation, we have carried out calculations of a sample boundary-value problem to test the applicability of the boundary distribution technique to such problems. For this purpose we have used $\psi(\mathbf{r}) = \cos(\pi x/2) \sin \gamma y$, where x and y are the components of $\mathbf{r}$, and $\gamma^2 + (\pi/2)^2 = \kappa^2$. This ψ is clearly a solution of the Helmholtz equation; because of the "mirroring" assumption made for $D(s)$, we must choose $\psi(\mathbf{r})$ to be an odd function of y. This solution was used to provide the specified boundary condition needed for Eq. (1), and the integral equation thereby obtained was solved using the techniques discussed earlier. In this inhomogeneous case, the solution for $D(s)$ has no arbitrariness and the resultant $\psi(\mathbf{r})$ can be compared directly with the analytic solution.

Calculations for the solution of this boundary value problem have been carried out for various values of κ near the interior and the exterior eigenvalues. The techniques

TABLE V

Results for Modified Treatment of the Inhomogeneous Case

κ	A	$\delta\psi_M$	$\delta\psi_U$
7.085	−2862.	0.185×10^{-4}	0.575×10^{-2}
7.09	−140.4	0.191×10^{-4}	0.300×10^{-3}
7.15	−11.15	0.127×10^{-3}	0.150×10^{-3}
7.15	−11.15	0.580×10^{-4}	0.150×10^{-3}
7.20	−6.235	0.112×10^{-4}	0.186×10^{-3}
7.25	−4.292	0.363×10^{-4}	0.190×10^{-2}
7.2549	−4.163	0.352×10^{-4}	0.305×10^{-1}

which were developed in I to eliminate the singularity in the solution as κ approaches an eigenvalue have been implemented quite successfully, both for the case in which the eigenvalue is associated with the exterior problem and for that in which it is associated with the interior one. A summary of the results is presented in Table V. Each calculation was carried out for an equilateral triangle for which $N_c = 5$, $N_d = 26$, and $h_f = 0.7$. The calculated values of the error in $\psi(\mathbf{r})$ at the center of the triangle for the modified and unmodified treatments are $\delta\psi_M$ and $\delta\psi_U$, respectively.

In I, the pole in $D(s)$ was isolated as κ approaches the eigenvalue, κ_0, by setting $D \equiv A\, D_0 + D_1$. If D_0 is the solution of the "partner" problem, A will have a pole as $\kappa \to \kappa_0$, but $\psi(\mathbf{r})$ will not. On the other hand, if D_0 is an eigensolution of the physical problem of interest, in some cases A may not be singular, as was discussed in I. In the upper part of Table V, we give results for calculations in which the integral equation was modified to eliminate the external eigensolution found at $\kappa_0 = 7.084742$, and it is found that the calculated value for A is well represented by $A = a/(\kappa - \kappa_0)$, where $a \simeq 0.738$. Further, as a representative value we give the error found for the unmodified ($\equiv \delta\psi_U$) and the modified ($\equiv \delta\psi_M$) treatments. It is seen that the error is greatly reduced by using the modified treatment as $\kappa \to \kappa_0$. In the lower part of the table, the modification involves the interior eigensolution for $\kappa_0 = 7.2552184$, where the boundary value problem does not in fact have a singularity. In these calculations, the further division of D_1 into Δ and δ as given by Eq. (I.30) was employed, and again it is seen that the accuracy achieved by the modification is substantial. In this latter case the simple division of D into D_0 and D_1 was also made, but calculated values for $\psi(\mathbf{r})$ were the same as in the unmodified treatment because the eigensolution, $\psi_0(\mathbf{r})$, is not zero inside the triangle and all terms must be included in Eq. (I.29). This calculation does give an alternative, but much poorer value for A. The error found for A in this way when multiplied by $(\mathbf{r}_0)$ produces most of the error obtained in the unmodified treatment for ψ. Finally, it may be noted that the value obtained for A is essentially the same for the physical or for the "partner"

eigensolution choice for D_0. This should not be surprising when it is recalled that, as shown in Fig. 4, the two eigensolutions are but little different.

V. Conclusion

In this article we have described techniques which have been developed for the solution of a singular integral equation which arises when a boundary dipole distribution is used to effect the solution of the Helmholtz equation for two-dimensional regions with sharp corners. These techniques make extensive use of analytic properties of the solution of the equation which were deduced in an earlier paper. In particular, these properties include the series of fractional powers or Bessel functions in terms of which the solution can be expanded in the vicinity of a corner, and regular behavior elsewhere on the sides.

Using these techniques we have obtained very accurate results for the eigenvalues of the Laplace operator for various two dimensional polygonal domains. In addition, we have a good indication from the ψ values calculated at extra points on the sides that the solution for ψ is quite accurate. We have shown that the series expansion for $D(s)$ is adequately convergent near a corner, with leading coefficients which are quite stable. We have also obtained accurate solutions of a sample Dirichlet boundary-value problem. Thus we feel that analytic properties can be very successfully invoked in obtaining satisfactory solutions for such equations.

Appendix A

In the numerical calculations the series of Eq. (7) was used directly for small (a/r). For larger ratios, the convergence of the series becomes very slow, so a modification was made to improve the convergence. Using the identity:

$$\frac{1}{n+\xi} = \frac{1}{n+a} + \frac{(a-\xi)}{(n+\xi)(n+a)},$$

we can obtain

$$\sum_{n=0}^{\infty} \frac{z^n}{n+\xi} = \sum_{n=0}^{\infty} \frac{z^n}{n+1} + (1-\xi) \sum_{n=0}^{\infty} \frac{z^n}{(n+1)(n+2)} + \cdots$$

$$+ (1-\xi)\cdots(k-\xi) \sum_{n=0}^{\infty} \frac{z^n}{(n+1)\cdots(n+k+1)}$$

$$+ (1-\xi)\cdots(k+1-\xi) \sum_{n=0}^{\infty} \frac{z^n}{(n+1)\cdots(n+k+1)(n+\xi)}.$$

Each of the series except the last can be obtained in analytic form, while the final

series converges rapidly because of the high power of n which appears in the denominator.

Appendix B

In the numerical analysis we have made comparisons with various analytic eigensolutions of Helmholtz' equation. The solutions for the square are well known. For the various triangles they are [8]:

Equilateral triangle

$$\psi(x, y) = \sin \frac{2\pi}{\sqrt{3}}(\sqrt{3}\, x + y) - \sin \frac{2\pi}{\sqrt{3}}(\sqrt{3}\, x - y) - \sin \frac{4\pi y}{\sqrt{3}}$$

$$\kappa = \frac{4\pi}{\sqrt{3}},$$

Isosceles right triangle

$$\psi(x, y) = \sin m\pi x \sin n\pi y - (-1)^{m+n} \sin n\pi x \sin m\pi y$$

$$\kappa = \pi(m^2 + n^2)^{1/2},$$

and

(30°–60°–90°) *triangle*

$$\psi(x, y) = \cos \frac{2\pi}{3}(5x + \sqrt{3}\, y) - \cos \frac{2\pi}{3}(5x - \sqrt{3}\, y)$$
$$+ \cos \frac{2\pi}{3}(-x - 3\sqrt{3}\, y) - \cos \frac{2\pi}{3}(-x + 3\sqrt{3}\, y)$$
$$+ \cos \frac{2\pi}{3}(-4x + 2\sqrt{3}\, y) - \cos \frac{2\pi}{3}(-4x - 2\sqrt{3}\, y)$$

$$\kappa = \frac{4\pi}{3}\sqrt{7}.$$

VI. Acknowledgment

The author would like to express his deep appreciation for the many lengthy, helpful discussions which he has had with Dr. Joseph V. Lepore throughout the work reported here. He would also like to thank Dr. Loren Meissner for many valuable conversations regarding various points in these calculations.

REFERENCES

1. R. J. RIDDELL, JR., *J. Computational Phys.* **31** (1979), 21–41.
2. M. ABRAMOWITZ AND I. A. STEGUN, "Handbook of Mathematical Functions," p. 360, Eq. (9.1.11), U. S. Government Printing Office, Washington, D.C., 1964.
3. A. ERDÉLYI, Ed., "Higher Transcendental Functions" Vol. I, Sec. 2.12, Eq. (1), McGraw–Hill, New York, 1953.
4. This result is easily obtained using Eqs. (9), (13), and (34) of Sec. 2.9 and Eq. (6) of Sec. 1.2 in Ref. [4].
5. L. FOX, P. HENRICI, AND C. MOLER, *SIAM J. Numer. Anal.* **4** (1967), pp. 80–102.
6. J. K. REID AND J. E. WALSH, *SIAM J. Appl. Math.* **13** (1965), pp. 837–850.
7. J. A. GEORGE, "Computer Science Implementation of the Finite Element Method," Report CS-208, Stanford University Computer Science Department, 1971.
8. G. C. NOONEY, "On the Vibrations of Triangular Membranes," Dissertation, Department of Mathematics, Stanford University, Stanford, Calif., Oct. 22, 1953.